October 2002

Synthesis and Dielectric Properties of $Li_{1-x+y}Ta_{1-x-3y}Ti_{x+4y}O_3$ *M*-Phase Solid Solutions

Albina Y. Borisevich
University of Pennsylvania

Peter K. Davies
University of Pennsylvania, davies@lrsm.upenn.edu

Copyright The American Ceramic Society. Reprinted from *Journal of the American Ceramic Society*, Volume 85, Issue 10, October 2002, pages 2487-2491.

Synthesis and Dielectric Properties of $Li_{1-x+y}Ta_{1-x-3y}Ti_{x+4y}O_3$ *M*-Phase Solid Solutions

Abstract

The synthesis, structure, and dielectric properties of the so-called *M*-phase solid solutions in the Li_2O-Ta_2O_5-TiO_2 system were investigated. Although the range of stability of the tantalate phases is more limited compared with their niobate counterparts, they have identical structures based on intergrowths of $LiTaO_3$-type blocks separated by corundum type layers. The dielectric constants of the tantalate *M*-phases range from 68 to 52 and they all exhibit a negative temperature coefficient of capacitance. The temperature coefficient of the resonant frequency measured in the microwave region can be tuned to zero, and the system shows quite good quality factors with the highest value reaching a $Q \times f = 10500$ at 6.7 GHz.

journal

J. Am. Ceram. Soc., 85 [10] 2487–91 (2002)

Synthesis and Dielectric Properties of $Li_{1-x+y}Ta_{1-x-3y}Ti_{x+4y}O_3$ *M*-Phase Solid Solutions

Albina Y. Borisevich* and Peter K. Davies*

Department of Materials Science and Engineering, University of Pennsylvania, Philadelphia, Pennsylvania 19104-6272

The synthesis, structure, and dielectric properties of the so-called *M*-phase solid solutions in the Li_2O–Ta_2O_5–TiO_2 system were investigated. Although the range of stability of the tantalate phases is more limited compared with their niobate counterparts, they have identical structures based on intergrowths of $LiTaO_3$-type blocks separated by corundum type layers. The dielectric constants of the tantalate *M*-phases range from 68 to 52 and they all exhibit a negative temperature coefficient of capacitance. The temperature coefficient of the resonant frequency measured in the microwave region can be tuned to zero, and the system shows quite good quality factors with the highest value reaching a $Q \times f = 10500$ at 6.7 GHz.

I. Introduction

In a recent paper[1] we reported on the synthesis, structure, and dielectric properties of the *M*-phase solid solution in the Li_2O–TiO_2–Nb_2O_5 system. These solid solutions, which have a general formula $Li_{1+x-y}Nb_{1-x-3y}Ti_{x+4y}O_3$ and a structure based on intergrowths of $LiNbO_3$-type blocks and $[Ti_2O_3]^{2+}$ corundum layers, have relative permittivities ranging from ~80 to ~55, tunable temperature coefficients, and quite low dielectric losses in the microwave region ($Q \times f$ up to 9000 at 6 GHz). In an attempt to modify the properties of these systems via chemical substitution, in this paper we report on the formation and dielectric properties of the corresponding tantalate solid solutions in the Li_2O–TiO_2–Ta_2O_5 system.

The phase behavior of in the Li_2O–TiO_2–Nb_2O_5 system was studied in detail by Villafuerte-Castrejon *et al.*,[2] who reported an extensive region of stability for the *M*-phase solid solution. For the corresponding tantalate system considerably less information is available. Several authors[3,4] have investigated selected quasi-binary sections and the extent of the $LiTaO_3$[5] and rutile[6] solid solution fields; however, no evidence was found for formation of an *M*-phase-type solid solution. For example, although the xLi_2TiO_3·$(1-x)LiNbO_3$ pseudobinary shows a limited range of *M*-phase stability for $0.1 \leq x \leq 0.3$,[7] the Li_2TiO_3–$LiTaO_3$ phase diagram is of a simple eutectic type with no intermediate compound formation. In contradiction to these reports, in a commentary on the phase stability of the Li_2O–TiO_2–Ta_2O_5 ternary Roth *et al.*[8] claimed that the tantalate system is similar to Li_2O–TiO_2–Nb_2O_5 and that a region of *M*-phase does occur, although no detailed experimental data were provided.

To resolve these apparent discrepancies in the literature one goal of this work was to confirm or deny the existence of the *M*-phase solid solutions in the Li_2O–TiO_2–Ta_2O_5 system and, if formed, determine their range of homogeneity. We also wished to investigate how the introduction of Ta would affect the microwave dielectric properties of the *M*-phases.

II. Experimental Procedure

Samples of the Ta *M*-phase solid solutions with $Li_{1+x-y}Ta_{1-x-3y}Ti_{x+4y}O_3$ were synthesized from dried Li_2CO_3 (Baker, 99.0%), Ta_2O_5 (Cerac, 99.95%), and TiO_2 (Cerac, 99.9%) powders. After mixing under acetone, the powders were preannealed at 700°C to drive off CO_2, and then reground and annealed in Pt crucibles at 1100°C for 10 h with subsequent ball-milling in ethanol. The annealing and ball-milling step was repeated until the XRD pattern of the resultant powder was either free of impurity peaks (2–5 times depending on the composition) or unchanged with heating time. Pellets were formed from the ball-milled powder, isostatically pressed at 80 000 psi, and sintered at 1125–1175°C for 1 h in Pt envelopes to prevent Li loss.

XRD patterns were collected on a Rigaku DMaxB diffractometer using Cu*K*α radiation generated at 45 kV and 30 mA. Data for lattice parameter refinements were collected at slow scan speeds. Peak positions for the lattice parameter refinements were determined by Lorentzian fit. Hexagonal cell parameters and an incommensurate parameter δ (where applicable) were refined simultaneously on an array of 22 to 27 fundamental reflections using a specially written program exploiting modified least-squares methods. Samples for TEM studies were prepared from pellets by conventional polishing, dimpling, and ion milling. Specimens were examined using a JEOL 2010F microscope operated at 200 kV.

The relative permittivity (ε_r, calculated from capacitance using room-temperature sample dimensions) and dielectric loss tangent (tan δ) were measured in the 100 Hz to 1 MHz frequency range from −100° to 200°C by the parallel-plate method using an HP 4284A precision LCR meter and a Delta 9920 environmental chamber. The temperature dependence of the capacitance in the range −20° to 80°C of all the samples was close to linear (correlation coefficients varying from 0.987 to 0.999), thus allowing reliable representation of the temperature coefficient of capacitance τ_c by a linear fit. The reproducibility of the dielectric measurements was controlled by using at least two separately prepared samples for each composition. Microwave measurements were performed via the cavity reflection method using a HP 8719C network analyzer. Ceramics with a height-to-diameter ratio = ~0.4 were placed into a gold-plated resonant cavity and their permittivities and *Q* values were calculated at the resonant conditions from the S_{11} reflection coefficients. The temperature coefficient of the resonant frequency (τ_f) was determined in the temperature range 0°–80°C by inserting the test cavities into a temperature-controlled chamber.

III. Results

The first goal of this investigation was to examine the stability range, if any, of *M*-phase-type solid solutions in the Li_2O–Ta_2O_5–TiO_2 system at 1100°C. Approximately 20 samples, formulated as

R. S. Roth—contributing editor

Manuscript No. 187588. Received July 16, 2001; approved February 15, 2002.
This project was supported by the National Science Foundation through Grant No. DMR98-09035. This work also made use of MRSEC Shared Experimental Facilities supported by the National Science Foundation under Award No. DMR 96-32598.
*Member, American Ceramic Society.

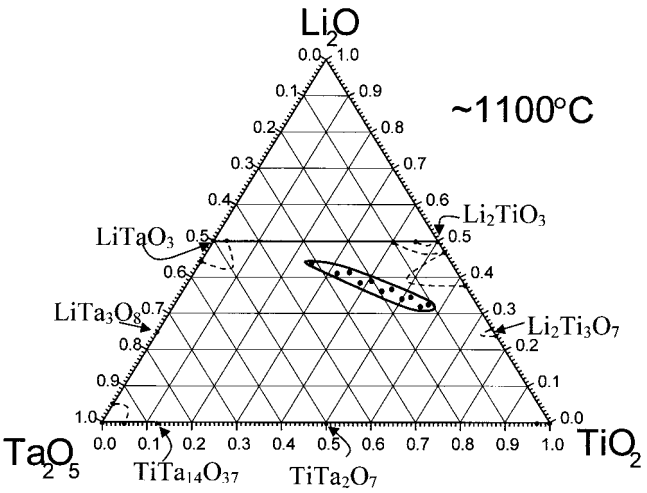

Fig. 1. Partial phase diagram for the Li_2O–Ta_2O_5–TiO_2 system at 1100°C: (solid line) *M*-phase field, (dashed lines) known single-phase fields.

$Li_{1+x-y}Ta_{1-x-3y}Ti_{x+4y}O_3$, were prepared with $0.05 \leq x \leq 0.2$, $0 \leq y \leq 0.2$. Following several heat treatments the single phase forming area of the *M*-phase solid solutions was established and is shown in Fig. 1. Compared with their niobate counterparts the tantalate *M*-phase field is considerably narrower and extends from $0.1 \leq x \leq 0.15$, $0.05 \leq y \leq 0.175$, with the $x = 0.15$, $y = 0.05$ point excluded. The observed region of stability lies below the Li_2TiO_3–$LiTaO_3$ pseudobinary and, in full agreement with Ref. 7, there was no evidence of any *M*-phase formation in the multiphase samples prepared along that join. Clearly the $LiTaO_3$–Li_2TiO_3–*M*-phase three-phase region is very small compared with its Nb analogue.

The XRD patterns of the Ta *M*-phases were indexed using fractional Miller indexes along the hexagonal *c* direction, a scheme first proposed by Roth and Davis;[8] attempts to index experimental data with the scheme proposed by Smith and West[9] were unsuccessful. The details of the indexing were described in a previous paper.[1] The X-ray patterns of the tantalate *M*-phases were almost identical to their Nb counterparts with the same *x* and *y* values. The high-order satellite peaks were weaker and broader, and in general no satellites above the second order were observed. These patterns contained $(h,k,4-2\delta)$ peaks (relative intensity 2%–5%) along with $(h,k,4+\delta)$; the former were completely invisible for the Nb system because of their low intensity.

The quantity $2/\delta$ in Roth's indexing scheme can be interpreted as the average number of layers $\langle n \rangle$ in the repeating block of each composition. It was demonstrated in our work on the niobate *M*-phases[10] that fractional values of $\langle n \rangle$ correspond to a mixture of two (or more) commensurate (integer $\langle n \rangle$) *M*-phases within the same sample. Because of the reduced intensity and larger width of the observed superstructure peaks for the Ta system typically it was not possible to reliably index the patterns with fractional $\langle n \rangle$ values as two-phase mixtures and instead the incommensurate formalism was used to interpret the XRD data. The refined cell parameters, the incommensurate parameter δ, and the mean block length $\langle n \rangle$ for all compositions within the *M*-phase field are summarized in Table I. The *a* and *c* subcell parameters change uniformly with composition and the incommensurate parameter δ increases (and the mean block length decreases) with increasing *y*.

To confirm the commensurate character of the Ta *M*-phases that to X-rays had a noninteger value of $\langle n \rangle$, electron diffraction and HRTEM studies of a tantalate sample with $x = 0.1$, $y = 0.175$ ($\langle n \rangle = 8.55$) were conducted. The [100] zone afforded the best orientation for observation of the cation sublattice as it is normal to *c**, the superstructure direction, and parallel to the direction in which the projected positions of cations are most easily resolved. As with the Nb *M*-phases,[10] the sample was found to comprise grains of different commensurate phases, in this case with 8- and 9-layer repeats. Figure 2 shows the [100] electron diffraction pattern for one of the 9-layer grains; the commensurate character of the pattern along the *c*-axis can be clearly discerned. The corresponding high-resolution TEM image (not shown) of the 9-layer grain revealed contrast from an 8-layer $LiNbO_3$-type block, separated by single layers of a different type. Detailed structure refinements and image analyses of the niobate phases have shown that the intermediate layer has a corundum-type structure.[10]

The dielectric properties of dense (≥93% theoretical) ceramics of the *M*-phase powders were measured at frequencies from 100 Hz to 1 MHz between −100° and 200°C. The sintering treatments were conducted between 1125° and 1172°C in platinum envelopes to avoid the loss of Li. The results for the relative permittivity and the temperature coefficient of the capacitance at 1 MHz are listed in Table II. The values listed in the table for the relative permittivity were corrected for the relative density and represent the average of two to three separately prepared samples of each composition. The observed relative permittivity values ranged from 68 ($x = 0.1$, $y = 0.075$) to 51 ($x = 0.1$–0.15, $y = 0.175$). The permittivity exhibits well-defined compositional trends and generally decreases with increasing *x* and *y*. It is evident from Table III that τ_c also varies strongly with composition ranging from ~−50 to ~−130 ppm/K. While all of the observed τ_c values were negative, many of them were low, suggesting that after the correction for thermal expansion ($\tau_f = -(\tau_c + \alpha_L)/2$) a zero τ_f could be expected. The dielectric loss, tan δ, was low ($\sim 10^{-4}$) or even negative, suggesting that precision of the measurement at 1 MHz was not sufficient to determine the actual loss of the ceramic.

Data for the microwave dielectric properties were collected for selected samples of the Ta *M*-phase solid solutions using the cavity reflection method. The values of the permittivity (78 to 55) at GHz frequencies (Table III) were in good agreement with those observed at 1 MHz. The temperature coefficient of the resonant frequency, τ_f, ranged from −5 to +32 ppm/K with a zero value being expected for samples with $x = 0.1$, $y \sim 0.08$ and $x \sim 0.11$, $y = 0.75$. The *Q* values, which are the reciprocal of the dielectric loss, increase with the titanium content reaching a $Q \times f$ of ~10 500 (at 6 GHz) for the sample with $x = 0.1$, $y = 0.175$.

Table I. Lattice Parameters for $Li_{1+x-y}Ta_{1-x-3y}Ti_{x+4y}O_3$ M-Phase Compositions

x	*y*	*a* (Å)	*c* (Å)	δ	$\langle n \rangle$
0.1	0.05	5.137(8)	13.819(1)	0.110(2)	18.14
0.1	0.075	5.130(5)	13.842(7)	0.151(3)	13.22
0.15	0.075	5.124(4)	13.851(6)	0.166(9)	11.98
0.1	0.1	5.124(7)	13.865(1)	0.187(5)	10.67
0.15	0.1	5.117(4)	13.870(7)	0.206(8)	9.67
0.1	0.125	5.113(7)	13.870(9)	0.205(0)	9.76
0.15	0.125	5.114(5)	13.902(6)	0.241(5)	8.28
0.1	0.15	5.098(8)	13.869(4)	0.216(2)	9.25
0.15	0.15	5.104(1)	13.919(0)	0.281(2)	7.11
0.1	0.175	5.099(2)	13.889(9)	0.233(8)	8.55
0.15	0.175	5.099(0)	13.930(5)	0.288(8)	6.93

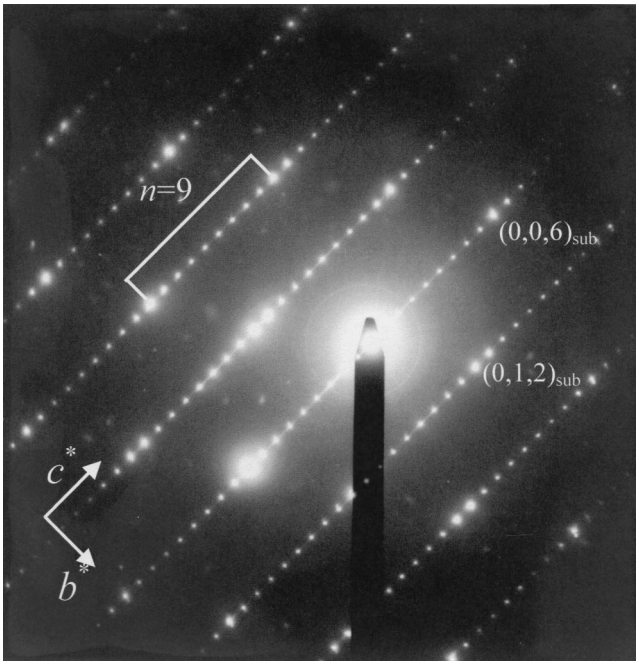

Fig. 2. Indexed [100] electron diffraction pattern for $Li_{0.925}Ta_{0.375}Ti_{0.8}O_3$ ($x = 0.1$, $y = 0.175$) 9-layer grain with lithium niobate subcell reflections indicated.

IV. Discussion

In agreement with the previous suggestions by Roth *et al.*,[8] the phase stability investigations in this study demonstrate that *M*-phase-type $Li_{1+x-y}Ta_{1-x-3y}Ti_{x+4y}O_3$ solid solutions can be formed in the Li_2O–Ta_2O_5–TiO_2 ternary system. However, the region of stability for the *M*-phase tantalates is significantly narrower than in the corresponding niobate system and there is no evidence for *M*-phase formation along the $LiTaO_3$–Li_2TiO_3 pseudobinary join. For the Nb system it is in this region of the phase diagram that the highest superstructure periodicities for the *M*-phase (up to 50 layers for the Nb system) were observed. Without additional information on the specific mechanisms responsible for the stabilization of the *M*-phase structure, the reasons for the difference in the compositional stabilities in the Ta and Nb systems are unclear.

The structural similarity of the *M*-phase Nb and Ta solid solutions was supported by analyses of XRD, electron diffraction, and HRTEM data. Qualitative simulations of the effect of the substitution of Ta on the powder XRD patterns were made using the atomic coordinates reported for the 5-layer and 10-layer niobate structures reported by Bordet *et al.*[11] and Farber *et al.*[10] The simulations demonstrated that minor differences in the satellite peak intensity in the Ta system could be fully explained by the different atomic scattering factors of Nb and Ta.

Table II. Dielectric Properties of $Li_{1+x-y}Ta_{1-x-3y}Ti_{x+4y}O_3$ at 1 MHz

x	y	ε_r (25°C)	τ_c (ppm/K)
0.1	0.075	67.7	−49
0.15	0.075	62.7	−50
0.1	0.1	59.4	−86
0.15	0.1	61.1	−98
0.1	0.125	54.1	−98
0.15	0.125	57.1	−117
0.1	0.15	53.6	−97
0.15	0.15	54.2	−137
0.1	0.175	51.5	−103
0.15	0.175	51.6	−126

Table III. Microwave Dielectric Properties of Selected Ta *M*-Phase Samples

x	y	f (GHz)	ε_r	τ_f (ppm/K)	Q	$Q \times f$ (GHz)
0.1	0.075	6.167	60.49	−5	813	5014
0.15	0.075	6.141	62.12	13	1008	6190
0.1	0.1	6.203	58.97	26	1282	7721
0.15	0.1	6.349	59.65	42	1435	9111
0.1	0.15	6.419	54.78	34	1621	10405
0.1	0.175	6.672	49.82	32	1578	10528

For the composition with $x = 0.15$, $y = 0.075$ the average layer repeat calculated from the XRD data ($\langle n \rangle = 11.98$) lies so close to an integer value that it can be reliably indexed as a single-phase 12-layer homologue. The indexing is shown in Table IV. To further validate the structural similarity of the Nb and Ta *M*-phases, our experimental pattern was compared with a theoretical pattern generated for an ideal atomic arrangement for a 12-layer homologue of H–Li_3TiO_3[11] with $a = 5.126$ Å, $c = 83.11$ Å. The space group (*R*-3), atom positions, Ta/Ti, and Li occupancies were chosen to conform to the overall stoichiometry ($Li_{1.075}Ta_{0.625}Ti_{0.45}O_3$) and the general crystallographic rules for the *M*-phases developed in Ref. 10. As is evident from Fig. 3, even without any attempt at refinement the resultant calculated pattern closely matches the experimental data.

The lattice parameters across the *M*-phase region follow essentially the same trends as those reported for the niobates with the *a* parameter decreasing linearly with *y* (Table I). Similar behavior is observed for the *c* subcell parameter (Table I). The mean block length decreases rapidly with increasing *y* and ranges from ~18 for $x = 0.1$, $y = 0.05$ to ~7 for $x = 0.15$, $y = 0.15$. When compared with the block lengths of Nb *M*-phases with the same composition, the Ta derivatives yielded consistently higher values (Fig. 4). The increased superlattice periodicity of the Ta *M*-phases can be attributed to a higher tolerance of the $LiTaO_3$ blocks to the substitution of Ti.

The dielectric properties of the Ta *M*-phases also behave similarly to those of the Nb derivatives, in both their absolute values and compositional trends. The effect of the changes in composition on the dielectric permittivities can be analyzed using

Table IV. Indexed Pattern for 12-Layer Structure of $Li_{1.075}Ta_{0.625}Ti_{0.45}O_3$ ($R - 3$, $a = 5.126$ Å, $c = 83.11$ Å)

$2\theta_{obs}$	$2\theta_{calc}$	I_{obs}	h	k	l	$l_{incommens}$[†]
21.74	21.75	2	0	1	8	$2 - 4\delta$
23.21	23.22	100	0	1	11	$2 - \delta$
25.02	25.02	41	0	1	14	$2 + 2\delta$
27.09	27.11	2	0	1	17	$2 + 5\delta$
31.05	31.06	5	1	0	22	$4 - 2\delta$
33.65	33.65	58	1	0	25	$4 + \delta$
34.98	34.98	43	1	1	0	0
38.98	38.98	4	0	0	36	6
40.21	40.21	9	1	1	18	3
42.41	42.41	14	2	0	11	$2 - \delta$
43.50	43.49	8	2	0	14	$2 + 2\delta$
47.48	47.47	3	0	2	22	$4 - 2\delta$
49.32	49.32	25	0	2	25	$4 + \delta$
53.37	53.37	34	1	1	36	6
56.08	56.10	18	1	2	11	$2 - \delta$
56.99	56.99	8	1	2	14	$2 + 2\delta$
59.33	59.32	6	0	1	50	$8 + 2\delta$
60.31	60.31	1	1	2	22	$4 - 2\delta$
61.89	61.89	16	1	2	25	$4 + \delta$
62.74	62.73	13	3	0	0	0
67.69	67.69	2	2	0	47	$8 - \delta$
70.77	70.76	3	2	0	50	$8 + 2\delta$
72.50	72.52	5	1	0	61	$10 + \delta$
73.89	73.89	4	2	2	0	0

[†] $l_{incommens}$ represents general indexing scheme for *M*-phases; see text and Refs. 1 and 8.

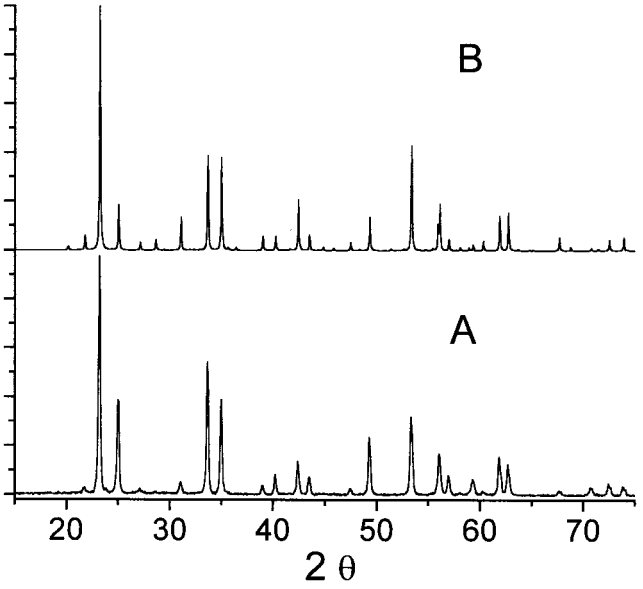

Fig. 3. Experimental XRD powder pattern for $Li_{1.075}Ta_{0.625}Ti_{0.45})_3$ (A) and theoretically generated pattern for 12-layer homologue of H–$Li_2Ti_3O_7$ with the same overall composition (B).

the dielectric polarizability, α_D, which eliminates the effect of the alterations in unit cell volume across the solid solution field. The polarizabilities were calculated using the Clausius–Mossotti equation (where $\alpha_D = (3/4\pi)V_m(\varepsilon_r - 1)/(\varepsilon_r + 2)$, V_m = molar volume = $V_{unit\ cell}/Z$). The plots of the polarizability for selected series of samples (Fig. 5) reveal a linear decrease in α_D with increasing y. The linear dependence of α_D on y implies that the permittivity of the *M*-phase can be described by simple empirical formalisms such as the ion additivity rule proposed by Shannon.[12] Thus the properties are primarily determined by bulk composition rather than by the lengths of the $LiTaO_3$ slabs or other structural characteristics.

It should be noted, however, that the total polarizability computed from the individual ion parameters tabulated by Shannon[11] did not agree with our experimental values. In particular, the experimental polarizabilities of the Nb phases were consistently higher than their Ta counterparts. By comparing the polarizabilities of Nb and Ta solid solutions with the same composition, we

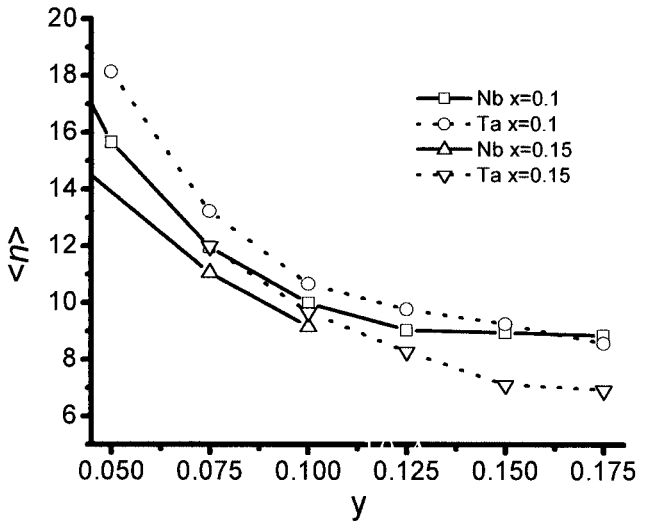

Fig. 4. Average block length ($\langle n \rangle$) versus composition for Nb and Ta *M*-phases.

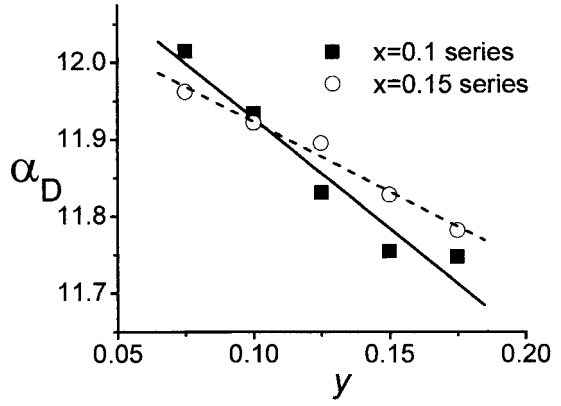

Fig. 5. Dielectric polarizability versus composition for $Li_{1+x-y}Ta_{1-x-3y}Ti_{x+4y}O_3$ *M*-phase solid solutions.

estimate that the ionic dielectric polarizability of Nb^{5+}, $\alpha_D(Nb)$, is 0.21 ($\pm$ 0.07 Å^3) higher than that of Ta^{5+}. This should be contrasted to the lower value ($\alpha_D(Nb) - \alpha_D(Ta) = -0.76$ Å^3) predicted by Shannon. The higher polarizability observed for Nb^{5+} in *M*-phase is consistent with the dielectric data reported for several other Ta^{5+} and Nb^{5+} systems in the literature (see, for example, Ref. 13).

The temperature coefficients of capacitance (τ_C) for the Ta *M*-phases at 1 MHz also exhibit systematic changes with composition. All of the values were negative (Table II), with samples with the highest Ti concentrations exhibiting the largest negative τ_C's. The microwave τ_f's follow a similar trend and, as with the Nb system, change sign within the phase field (Table III). A zero τ_f can be expected for $x = 0.1$, $y \sim 0.08$ and for $x \sim 0.11$, $y = 0.75$. It should be noted that the values of linear thermal expansion coefficient α, if calculated from τ_C's and τ_f's, are high (up to 59 ppm/K) and change irregularly within the *M*-phase field. The former could be an indication of the frequency dependence of the temperature coefficient; the latter may reflect uncertainties in the value of τ_f, which was calculated from considerably fewer data points as compared with τ_C. An estimate of the thermal expansion coefficient in this system cannot be made reliably without direct measurement; $LiTaO_3$, for example, exhibits considerable anisotropy of thermal expansion with α_a of ~8 ppm/K and α_c of ~−13 ppm/K.[14]

The microwave quality factors Q (Table III) exhibit uniform changes with composition and increase in the y direction. This change parallels the decrease in permittivity. The highest Q value was observed for $x = 0.1$, $y = 0.175$ ($Q \times f = 10500$) while the composition closest to a zero τ_f has $\varepsilon_r \sim 60$, $Q \times f \sim 5000$.

V. Conclusions

We have confirmed that $Li_{1+x-y}Ta_{1-x-3y}Ti_{x+4y}O_3$ *M*-phase type solid solutions can be formed in the Li_2O–Ta_2O_5–TiO_2 system at 1100°C. Our studies indicate that the Nb and Ta *M*-phases are essentially isostructural. The lattice parameters exhibit trends similar to those observed for the Nb system and the XRD data indicate a somewhat higher overall solubility of Ti^{4+} in the $LiTaO_3$ slabs compared with $LiNbO_3$.

Ceramics with high relative densities were obtained by sintering the obtained powders at 1125–1175°C. The relative permittivities of Ta *M*-phase samples have values ranging from 68 to 52. The temperature coefficients of capacitance at 1 MHz are negative and increase in absolute value with increasing y. The temperature coefficient of the resonant frequency measured in the microwave region exhibits tunability to zero. The system shows quite good quality factors at microwave frequencies with the highest value reaching a $Q \times f = 10500$ at 6.7 GHz.

Acknowledgments

We thank L. Farber for collecting the TEM data and M. Valant for microwave measurements.

References

[1]A. Y. Borisevich and P. K. Davies, "Crystalline Structure and Dielectric Properties of $Li_{1+x-y}Nb_{1-x-3y}Ti_{x+4y}O_3$ *M*-Phase Solid Solutions," *J. Am. Ceram. Soc.*, **85** [3] 573–78 (2002).

[2]M. E. Villafuerte-Castrejon, A. Aragon-Pina, R. Valenzuela, and A. R. West, "Compound and Solid Solution Formation in the System Li_2O–Nb_2O_5–TiO_2," *J. Solid State Chem.*, **71**, 103–108 (1987).

[3]L. C. Martel and R. S Roth, *Am. Ceram. Soc. Bull.*, **60** [3] 376–76 (1981). (Cited in R. S. Roth (ed.), *Phase Equilibria Diagrams*, Vol. 11; p. 232. American Ceramic Society, Westerville, OH, 1995.)

[4]Q. M. Shu, Y. P. Chen, H. C. Xia, Y. D. Jiang, T. X Gu, and Q. S Zhao, *Rengong Jingti*, **16** [2] 94–100 (1987). (Cited in R. S. Roth (ed.), *Phase Equilibria Diagrams*, Vol. 11; p. 233. American Ceramic Society, Westerville, OH, 1995.)

[5]B. Elouadi, M. Zriouil, J. Ravez, and P. Hagenmuller, "Some New Non-stoichiometric Ferroelectric Phases Appearing Close to $LiTaO_3$ in the Ternary System Li_2O–Ta_2O_5–TiO_2," *Mater. Res. Bull.*, **16**, 1099–106 (1981).

[6]J. A. Garcia, M. E. Villafuerte-Castrejon, J. Andrade, R. Valenzuela, and A. R. West, "New Rutile Solid Solutions, $Ti_{1-4x}Li_xM_{3x}O_2$: M = Nb, Ta, Sb," *Mater. Res. Bull.*, **19**, 649–54 (1984).

[7]M. E. Villafuerte-Castrejon, J. A. Garcia, E. Cisneros, R. Valenzuela, and A. R. West, "Phase Equilibria in the Systems Li_2TiO_3–$LiNbO_3$, Li_2TiO_3–$LiTaO_3$, and Li_2TiO_3–$LiNbO_3$–$LiTaO_3$," *Br. Ceram. Trans. J.*, **83** [5] 143–45 (1984).

[8]R. S. Roth and K. L. Davis, "Incommensurate Solid Solution in TiO_2 Doped $LiNbO_3$ and $LiTaO_3$"; p. 88 in *ACerS Annual Meeting, 89th*. American Ceramic Society, Westerville, OH, 1987. Also in R. S. Roth (ed.), *Phase Equilibria Diagrams*, Vol. 11; pp. 231–32. American Ceramic Society, Westerville, OH, 1995.

[9]R. I. Smith and A. R. West, "Characterization of an Incommensurate LiTiNb Oxide," *Mater. Res. Bull.*, **27**, 277–85 (1992).

[10]L. Farber, I. Levin, A. Borisevich, I. E. Grey, R. S. Roth, and P. K. Davies, **"**Structural Study of $Li_{1+x-y}Nb_{1-x-3y}Ti_{x+4y}O_3$ Solid Solutions," *J. Solid State Chem.*, **166**, 81–90 (2002).

[11]P. Bordet, C. Bougerol-Chaillout, I. Grey, J. L. Hodeau, and O. Isnard, "Structural Characterization of the Engineered Scavenger Compound, H–$Li_2Ti_3O_7$," *J. Solid State Chem.*, **152**, 546–53 (2000).

[12]R. D. Shannon, "Dielectric Polarizability of Ions in Oxides and Fluorides," *J. Appl. Phys.*, **73** [1] 348–66 (1993).

[13]H. C. Ling, M. F. Yan, W. W. Rhodes, "Phase Stability in $Pb(B'_{1/2}{}^{3+}B''_{1/2}{}^{5+})O_3$ and $Pb(B'_{1/3}{}^{2+}B''_{2/3}{}^{5+})O_3$ Compositions," *Ferroelectrics*, **89**, 69–80 (1989).

[14]K.-H. Hellwege and A. M. Hellwege (eds.), *Landolt-Bornstein New Series*, Vol. 16a; p. 359. Springer-Verlag, Berlin, Germany, 1981. □